Proceedings of the 2002 IEEE
International Conference on Robotics & Automation
Washington, DC • May 2002

The BlueDRAGON - A System for Measuring the Kinematics and the Dynamics of Minimally Invasive Surgical Tools In–Vivo

Jacob Rosen (1), Jeffrey D. Brown (2), Lily Chang (3), Marco Barreca (3), Mika Sinanan (3,1), Blake Hannaford (1,3)

(1) Department of Electrical Engineering, Box 352500,University of Washington, Seattle, WA
(2) Department of Bioengineering, Box 352500, University of Washington, Seattle, WA
(3) Department of Surgery, Box 356410, University of Washington, Seattle, WA

<rosen, jdbrown, lchang, mbarreca, mssurg, blake> @u.washington.edu
Biorobotics Lab: http://brl.ee.washington.edu - Center of Videoendoscopic Surgery: http://depts.washington.edu/cves/

ABSTRACT

Minimally invasive surgery (MIS) involves a multi-dimensional series of tasks requiring a synthesis between visual information and the kinematics and dynamics of the surgical tools. Analysis of these sources of information is a key step in mastering MIS but may also be used to define objective criteria for characterizing surgical performance. The BlueDRAGON is a new system for acquiring the kinematics and the dynamics of two endoscopic tools along synchronized with the visual view of the surgical scene. It includes two four-bar passive mechanisms equipped with position and force torque sensors for measuring the positions and the orientations (P/O) of two endoscopic tools along with the forces and torques (F/T) applied by the surgeon's hands. The methodology of decomposing the surgical task is based on a fully connected, 28 finite-states Markov model where each states corresponded to a fundamental tool/tissue interaction based on the tool kinematics and associated with unique F/T signatures. The experimental protocol included seven MIS tasks performed on an animal model (pig) by 30 surgeons at different levels of their residency training including expert surgeons. Preliminary analysis of these data showed that major differences between residents at different skill levels were: (*i*) the types of tool/tissue interactions being used, (*ii*) the transitions between tool/tissue interactions being applied by each hand, (*iii*) time spent while performing each tool/tissue interaction, (*iv*) the overall completion time, and (*v*) the variable F/T magnitudes being applied by the subjects through the endoscopic tools. Systems like surgical robots or virtual reality simulators that inherently measure the kinematics and the dynamics of the surgical tool may benefit from inclusion of the proposed methodology for analysis of efficacy and objective evaluation of surgical skills during training.

1. INTRODUCTION

The use of minimally invasive surgical (MIS) techniques has become widespread only within the last ten years, due to the fact the only recently has the instrumentation developed to an extent that makes the performance of laparoscopic general surgical procedures possible. Using a miniature video camera and instruments inserted through small portals, operations previously performed through large incisions that required long recovery times are now performed with a much shorter recovery and lessen the chance of infection to the patient. However from surgeon perspective, the use of this new technology has required a new set of skills due to its new human-machine interface.

Performing MIS involves a multi-dimensional series of tasks requiring a synthesis between visual information and the kinematics and dynamics of the surgical tools. One of the more difficult tasks in surgical education is to teach and objectively assess the optimal application of instrument forces and torques and the associated tools' kinematics necessary to conduct an operation. This is especially problematic in the field of MIS where the teacher is one step removed from the actual conduct of the operation.

Along with the progress in developing MIS techniques, two additional modalities emerged in the last decade including teleoperated surgical robots and virtual reality simulators incorporating haptic technology as preoperative training tool. All these three modalities associated with MIS shared the same user interface in which both visual and kinesthetic information is flowing at the interface between the surgeon and the tools. Analysis of these sources of information is a key step in decomposing MIS surgery into its primary elements. The task decomposition can also be used to define objective criteria for characterizing surgical performance that is currently assessed by subjective methods in the operating room or applied when reviewing a video-tape of the surgery.

The proposed methodology for objective assessment of technical skill in MIS is based on the kinematics and the dynamics of the surgical tools measured at the tool/hand interface. The power of this methodology arises from decomposing the surgical task into its fundamental

elements, and therefore it is independent from the modality being used (in-vivo surgery, robotic surgery or virtual reality simulators).

Pervious research focused on measurement and analysis of the forces and torques being applied by the surgeons on a single endoscopic tool during two common laparoscopic procedures: cholecystectomy and Nissen fundoplication [1, 2].. In addition, Markov models were used to analyze and predict the skill level of the surgeon, based solely on the forces and torques they apply.

The aim of the study was to develop a system of acquiring data in a real MIS setup and a methodology for decomposing two handed surgical tasks using Markov models (MM) based on the kinematics and the dynamics of the surgical tools. These models enable objective assessment of surgical skills.

2. TOOLS AND METHODES

2.1 The BlueDRAGON System

The BlueDRAGON is a system for acquiring the kinematics and the dynamics of two endoscopic tools along with the visual view of the surgical scene (Fig. 1). The system includes two four-bar passive mechanisms attached to endoscopic tools [4]. The endoscopic tool in a minimal invasive surgery is inserted into the body through port located for example in the abdominal wall. The tool is rotated around pivot point inside the port that is inaccessible for sensors aimed to measure the tool's rotation. The four bar mechanism translates the tool's rotation into virtual pivot points elsewhere on the mechanism. These translation is enabled when the base axes and the tool's shaft axis intersect the port's pivot point (Figure 2). The tool's movements in the port are then tracked by sensors that are incorporated into the mechanism's joints. Moreover, the mechanism's axes alignment prevented any additional moments applied on the skin and internal tissues except the ones that are generated intentionally by using the tools. The mass of the mechanism's moving parts is 1.36 kg and its maximal moment of inertia relative to the X- axis (I_{xx}) depicted in Fig. 2 is 0.157 Kgm^2. However, the gravitational forces applied on the surgeon's hand when the mechanism is placed away from its neutral position are compensated by an optimized spring connecting the base with the first two coupled links.

The two mechanisms are equipped with three classes of sensors: (i) position sensors (multi turn potentiometers - Midori America Corp.) are incorporated into four of the mechanisms' joints for measuring the positions, the orientations and the translation of the two instrumented endoscopic tools attached to them. In addition, two linear potentiometer (Penny & Giles Controls Ltd.) that are attached to the tools' handles are used for measuring the endoscopic handle and tool tip angles; (ii) three-axis force/torque (F/T) sensors (ATI-Mini sensor) are located at the proximal end of the endoscopic tools' shafts, as well as force sensors inserted into the tools' handles for measuring the grasping forces at the hand/tool interface and (iii) contact sensors providing binary indication of any tool/tissue contact.

Figure 1: *The BlueDRAGON system integrated into a minimally invasive surgery operating room*

Data measured by the BlueDRAGONs' sensors are acquired using two 12-bit National Instruments USB A/D cards sampling the 26 channels (3 rotations, 2 translations, 1 tissue contact, and 7 channels of forces and torques from each instrumented grasper) at 30 Hz. In addition to the data acquisition, the synchronized view of the surgical scene is incorporated into a graphical user interface displaying the data in real-time.

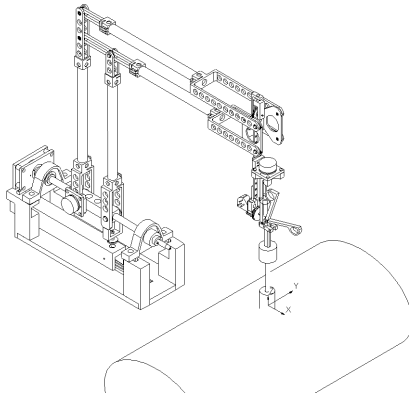

Figure 2: *CAD drawing of the BlueDRAGON mechanism and its coordinate system.*

2.2 MIS Task Decomposition

The methodology of decomposing surgical task is based a fully connected, symmetric finite-states (28 states) MM where the left and the right hands are represented by 14 states each (Figure 3). Each one of the 14 states corresponded to a fundamental tool/tissue interaction based on the tool kinematics and associated with unique F/T signatures defined as observations and measured at the hand/tool interface (Table 1). In view of this model, any MIS task can be described as a series of finite state. In each state the surgeon is applying a specific F/T signature, out of several F/T signatures which are typical to that state, on the tissue by using the tool. The surgeon may stay at that state for specific time duration applying different F/T signatures associated with that state and then perform a transition to another state. The surgeon may utilize any of the 14 states by the using the left and the right tools independently. However, the states representing the tool/tissue interactions of the left and the right tools are mathematically and functionally linked.

The 14 tool/tissue interactions can be further divided into three types based on the number of movements performed simultaneously (Table 1). The fundamental maneuvers are defined as Type I. The 'idle' state is defined as moving the tool in space (abdominal cavity) without touching any internal organ. The forces and torques developed during this state represente mainly the interaction with the port and the abdominal wall, in addition to the gravitational and inertial forces of the tool. In the 'grasping' and 'spreading' states, compression and tension are applied to the tissue by closing and opening the grasper handle, respectively. In the 'pushing' state, the tissue is compressed by moving the tool along the Z axis. 'Sweeping' consists of placing the tool in one position while rotating it around the X and/or Y axes (port frame). The rest of the tool/tissue interactions in Types II and III are combinations of the fundamental ones defined as Type I.

The MM is defined by the compact notation (7). Each Markov sub model representing the left and the right tool is defined by λ_L and λ_R (Eq. 1). The sub model is defined by:

(i) The number of states - N whereas individual states are denoted as $S=\{s_1,s_1,\ldots s_N\}$, and the state at time t as q_t.;

(ii) The number of distinct observation symbol - M whereas individual symbols are denoted as $V=\{v_1,v_1,\ldots v_M\}$

(iii) The state transition probability distribution matrix – $A=\{a_{ij}\}$, where

$$a_{ij}=P[q_{t+1}=s_j \mid q_t=s_i] \qquad 1\le i,j\le N$$

(iv) The observation symbol probability distribution matrix – $B=\{b_j(k)\}$, where for state j

$$b_j(k)=P[v_k \text{ at } t \mid q_t=s_j] \qquad 1\le j\le N, 1\le k\le M$$

(v) The initial state distribution vector– π.

$$\pi_i=P[q_1=s_i] \qquad 1\le i\le N$$

The two sub models are linked to each other by the left-right interstate transition probability distribution matrix – $C=\{c_{lr}\}$, where

$$c_{lr}=P[q_{tL}=s_l \cap q_{tR}=s_r] \qquad 1\le l,r\le N$$

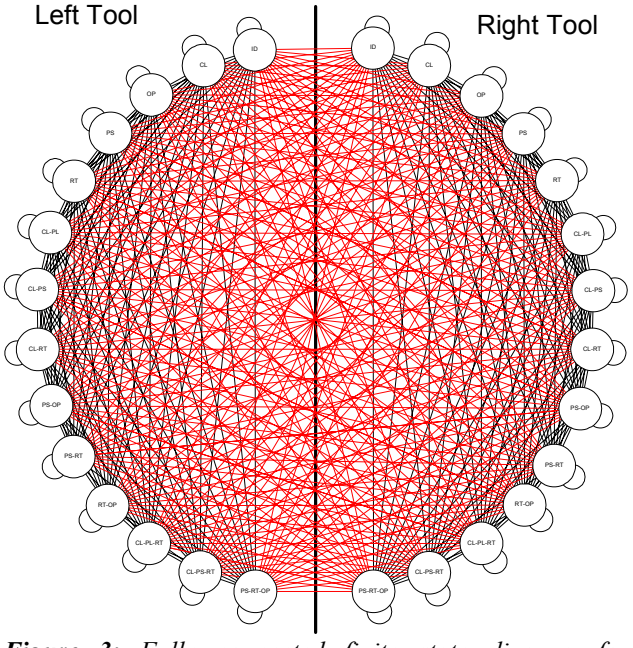

Figure 3: *Fully connected finite state diagram for decomposing MIS. The tool/tissue interactions of the left and the right endoscopic tools are represented by the 14 fully connected sub models. Circles represent states whereas lines represent transitions between states. Lines that cross the center line represent different combination of states. Force/torque signature associated with each state were omitted for simplifying the diagram.*

The probability observing the state transition $Q=\{q_1,q_2,\ldots q_T\}$ and the associated observation sequence $O=\{o_1,o_2,\ldots o_T\}$ given the two MM sub models (Eq. 1) and interstate transition probability distribution matrix is defined by Eq. 2a

$$\lambda_L=(A_L,B_L,\pi_L) \qquad \lambda_R=(A_R,B_R,\pi_R) \tag{1}$$

$$P(Q,O\mid\lambda_L,\lambda_R,C)=\pi_{q_L}\pi_{q_R}\prod_{t=0}^{T} a_{q_lq_{l+1}L}b_{q_tL}(o_t)a_{q_lq_{l+1}R}b_{q_tR}(o_t)c_{q_{tL}q_{tR}} \tag{2}$$

Due to the fact that probabilities by definition have numerical value in the range of 0 to 1. For relatively short time duration the probability calculated by Eq. 2 converge exponentially to zero and therefore exceed the precision range of essentially any machine. Hence by using

logarithmic transformation the resulting values of Eq. 2 in the range of [0 1] are mapped by eq. 3 into [- ∞ 0].

$$Log(P(Q,O \mid \lambda_L, \lambda_R, C)) = Log(\pi_{q_L}) + Log(\pi_{q_R}) + \sum_{t=1}^{T} Log(a_{q_t q_{t+1} L}) + Log(b_{q_t L}(o_t)) + Log(a_{q_t q_{t+1} R}) + Log(b_{q_t R}(o_t)) + Log(c_{q_t L q_t R}) \quad (3)$$

Once the MMs were defined for specific subjects with specific skill levels, it is then possible to calculate the statistical distance between them. This statistical distance is considered to be an objective criterion for evaluation of skill level if for example the statistical distance between a subject under study and an expert is being calculated. Given two MMs λ_1 and λ_2 the statistical distances between them $D(\lambda_1, \lambda_2)$ and $D(\lambda_2, \lambda_1)$ are defined by Eq. 4

$$D(\lambda_1, \lambda_2) = \frac{1}{T_{O_2}}[logP(O_2, Q_2 \mid \lambda_1) - logP(O_2, Q_2 \mid \lambda_2)] \quad (4)$$

$$D(\lambda_2, \lambda_1) = \frac{1}{T_{O_1}}[logP(O_1, Q_1 \mid \lambda_1) - logP(O_1, Q_2 \mid \lambda_2)]$$

$D(\lambda_1, \lambda_2)$ is a measure of how well model λ_1 matches observations and state sequence generated by model λ_2 relative to how well model λ_2 matches observations and state sequence generated by itself whereas T_{O_1} , and T_{O_2} stand for the time duration of the observation vectors O_1 and O_2 respectively. Since $D(\lambda_1, \lambda_2)$ and $D(\lambda_2, \lambda_1)$ are nonsymmetrical, The natural expression of the symmetrical statistical distance version is defined by Eq 5.

$$D_S(\lambda_1, \lambda_2) = \frac{D(\lambda_1, \lambda_2) + D(\lambda_2, \lambda_1)}{2} \quad (5)$$

2.3 Experimental Protocol

The experimental protocol included seven standard MIS tasks performed in-vivo on an animal model (pig) by 30 surgeons at different levels of their residency training (5xR1,R2,R3,R4,R5 where the numeral denotes year of training and 5 Expert Videoendoscopic surgeons). The surgical tasks were: (1) Running the bowel right to left; (2) Running the bowel left to right (3) Dissecting Mesenteric Arteries; (4) Passing a Suture; (5) Tying a Knot; (6) Suturing the Colon; and (7) Passing Stomach behind the Esophagus. All animal procedures were performed in an AALAC-accredited surgical research facility under an approved protocol from the institutional animal care committee of the University of Washington.

3. RESULTS

Typical raw data of forces torques and tool tip position were plotted in a 3D graphs showing the kinematics and the dynamics of the left and the right endoscopic tools measured by the BlueDRAGON while examining 0.762m of the bowel (Fig. 4).

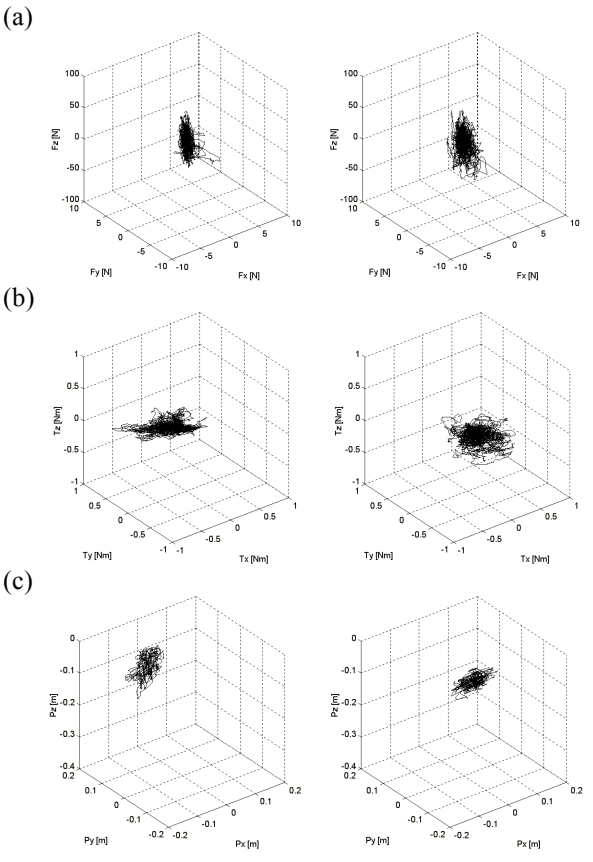

Figure 4: *The kinematics and dynamics data of the left and the right endoscopic tools measured by the Blue DRAGON while sequentially examining sections of the bowel (For coordinate system definition see Fig. 2) - (a) Forces; (b) Torques (c) Tool tip position.*

The forces and torques can be described as vectors with an origin at the center of the sensor and a coordinate system aligned with the tool coordinate system. These vectors are constantly changing both their magnitudes and orientations as a result of the F/T applied by the surgeon's hand on the tool while interacting with the tissues. The F/T as vectors can be depicted as arrows attached to the origin that are changing their lengths and orientations as a function of time. Fig.4a,b describes the traces of the tips of these vectors as they were changing during the surgical procedure. In a similar fashion the traces of the tool tips position were plotted in Fig 4c.

The forces along the Z axis (in/out of the port) were higher compared to the forces in the XY plane. On the other hand, torques developed by rotating the tool around the Z axis were extremely low compared to the torques generated while rotating the tool along the X and Y axis while sweeping the tissue or performing lateral retraction. Similar trends in terms of the F/T magnitude ratios between the X, Y, and Z axes were found in the data

measured in other MIS tasks. These raw data demonstrated the complexity of the surgical task. Profound understanding of the MIS task is gained by decomposing it to its prime elements.

A cluster analysis using the K-means algorithm was preformed for defining typical F/T signatures in the database. Figure 5 depicted 9 cluster centers identified in the data associated with the state defined by Grasping-Pushing-Sweeping. Similar F/T signatures associated with different states were then used to decode the entire database into discrete symbols.

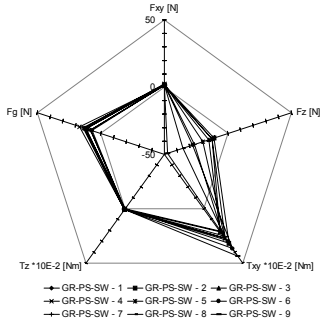

Figure 5: *Nine Force/Torque signatures (observations) obtained by cluster analysis of the data measured at the human/tool interface and associated with state defined as grasping-pushing-sweeping*

This decoding process allowed to decompose the surgical task and to depict it as a finite state diagram. A typical state transition (right hand tool) of tissue dissection performed in MIS was plotted in Fig. 6. The finite state diagram was constructed from two separate models representing the expert surgeon's model (ES) (solid line and dashed line) and the novice surgeon's model (R1) (solid line and dotted line).

The Idle state is the only state connected to all the other states in the diagram (Fig. 6). This state, in which no tool/tissue interaction was performed, was mainly used by both expert and novice surgeons to move from one operative state to the other. However, the expert surgeons used the idle state only as a transition state while the novices spent a significant amount of time in this state planning the next tool/tissue interaction. Another major difference between surgeons from different skill groups was related to the tool/tissue interaction and tool/tissue transitions used by these two groups. Surgeons took different paths to reach the same goal. Each group utilized states and transitions not used by the other group.

Further analysis of the F/T associated with each state showed that the F/T magnitudes were found to be task dependent. High F/T magnitudes were applied by novices compared to experts during tissue manipulation, and vice versa during tissue dissection. High efficiency of surgical performance was demonstrated by the expert surgeons and expressed by shorter tool tip displacements, shorter periods of time spent in the 'idle' state, and sufficient application of F/T on the tissue to safely accomplish the task.

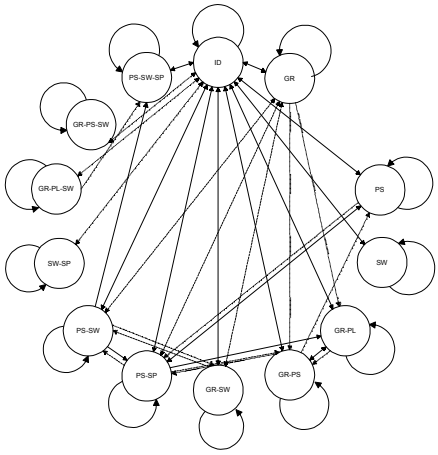

Figure 6: *Finite state diagram of MIS tissue dissection preformed by using endoscopic tool held by the right hand (Dashed line - transitions preformed by an expert surgeons - ES, Dotted line - transitions preformed by novice surgeons - first year residences R1, Solid line - transitions preformed both by R1 and ES)*

4. DISCUSSION

Minimally invasive surgery is a complex task that requires a synthesis between visual and kinesthetic information. Analyzing MIS in terms of these two sources of information is a key step towards developing objective criteria for training surgeons and evaluating the performance in different modalities including real surgery, master/slave robotic systems or virtual reality simulators incorporating haptic technology.

In developing the BlueDRAGON system several alternatives were examined as a 3D position tracking system including systems that are based on optical, acoustic, electromagnetic, and mechanical sensors. Considering the surgical scene with multiple instruments that might block the line of sight required by optical and acoustic systems, and the massive amount of metallic devises that might generate magnetic interference to the electromagnetic systems, a mechanical system utilizing a passive mechanism incorporating linear and rotary potentiometers and attached to the surgical tool provides a simple and robust solution for tracking the position and the orientations of the surgical tool.

The Markov model proved to be a very powerful method encompassing multi modal sources of information into compact mathematical representation of a complex task such as surgery. Moreover, once the model's architecture is determined and the model's parameters are calculated it provides quantitative and objective measure of surgical performance. A feasible analogy to the proposed methodology for decomposing the surgical task is the human language. Based on this analogy the basic states - tool/tissue interactions are equivalent to '*words*' of the MIS '*language*' and the 14 states are forming the MIS '*dictionary*'. In the same way as a single word is pronounced differently by different people, the same tool/tissue interaction is performed differently by different surgeons while applying different F/T magnitudes, yet they all share the same meaning, or outcome, as in the realm of surgery. The cluster analysis was used to identify the typical F/T associated with each one of the tool/tissue interactions in the surgery '*dictionary*', or using the language analogy, it characterized different pronunciations of a word. Utilizing the '*dictionary*' of surgery, the MM was then used to define the process of each task or step of the surgical procedure, or in other words, '*dictating chapters*' of the surgical '*story*'. The proposed methodology regains its power by decomposing the surgical task to its prime elements - tool/tissue interactions. These elements are inherent in MIS and they are independent for the modality being used.

ACKNOWLEDGMENTS - This research was funded by a major grant from US Surgical, a division of Tyco, Inc. to the University of Washington, Center for Videoendoscopic Surgery and a gift from Washington Research Foundation Capital.

REFERENCES

[1] Richards, C., Rosen, J., Hannaford, B., MacFarlane, M., Pellegrini, C., Sinanan, M., "Skills Evaluation in Minimally Invasive Surgery Using Force/Torque Signatures," Surg. Endosc., 14(9):791-8.

[2] Rosen J., Solazzo, M., Hannaford, B., Sinanan, M., 2001, "Objective Laparoscopic Skills Assessments of Surgical Residents Using Hidden Markov Models Based on Haptic Information and Tool/Tissue Interactions," Stud. Health Tech. Inform. 81:417-23.

[3] Rosen J., B. Hannaford, Richards C., M. Sinanan, Markov Modeling of Minimally Invasive Surgery Based on Tool/Tissue interaction and Force/Torque Signatures for Evaluating Surgical Skills, IEEE Transactions on Biomedical Engineering Vol. 48. No. 5, pp. 579-591 May 2001.

[4] Madhani, A.J., Niemeyer, G., Salisbury, J.K., Jr., 1998, "Black Falcon: A Teleoperated Surgical Instrument For Minimally Invasive Surgery," Proceedings, 1998 IEEE/RSJ International Conference on Intelligent Robots and Systems. Part 2:936-44.

Type	No.	State Name	State Acronym	Tissue Contact	Position / Orientation					Force / Torque						
					$\theta_x, \dot{\theta}_x$	$\theta_y, \dot{\theta}_y$	$\theta_z, \dot{\theta}_z$	$L_z, \dot{L}_z$	$\theta_g, \dot{\theta}_g$	F_x	F_y	F_z	T_x	T_y	T_z	F_g
I	1	Idle	ID	-	$\pm\varepsilon_{\dot{\theta}_x}$	$\pm\varepsilon_{\dot{\theta}_y}$	$\pm\varepsilon_{\dot{\theta}_z}$	$\pm\varepsilon_{\dot{L}_z}$	$\pm\varepsilon_{\dot{\theta}_g}$	$\pm\varepsilon_{F_x}$	$\pm\varepsilon_{F_y}$	$\pm\varepsilon_{F_z}$	$\pm\varepsilon_{T_x}$	$\pm\varepsilon_{T_y}$	$\pm\varepsilon_{T_z}$	$\pm\varepsilon_{F_g}$
	2	Closing Handle (Grasping / Cutting)	CL	+	$\pm\varepsilon_{\dot{\theta}_x}$	$\pm\varepsilon_{\dot{\theta}_y}$	$\pm\varepsilon_{\dot{\theta}_z}$	$\pm\varepsilon_{\dot{L}_z}$	$\dot{\theta}_g > \varepsilon_{\dot{\theta}_g}$	$\pm\varepsilon_{F_x}$	$\pm\varepsilon_{F_y}$	$\pm\varepsilon_{F_z}$	$\pm\varepsilon_{T_x}$	$\pm\varepsilon_{T_y}$	$\pm\varepsilon_{T_z}$	$F_g > \varepsilon_{F_g}$
	3	Opening Handle (Spreading)	OP	+	$\pm\varepsilon_{\dot{\theta}_x}$	$\pm\varepsilon_{\dot{\theta}_y}$	$\pm\varepsilon_{\dot{\theta}_z}$	$\pm\varepsilon_{\dot{L}_z}$	$\dot{\theta}_g < -\varepsilon_{\dot{\theta}_g}$	$\pm\varepsilon_{F_x}$	$\pm\varepsilon_{F_y}$	$\pm\varepsilon_{F_z}$	$\pm\varepsilon_{T_x}$	$\pm\varepsilon_{T_y}$	$\pm\varepsilon_{T_z}$	$F_g < -\varepsilon_{F_g}$
	4	Pushing	PS	+	$\pm\varepsilon_{\dot{\theta}_x}$	$\pm\varepsilon_{\dot{\theta}_y}$	$\pm\varepsilon_{\dot{\theta}_z}$	$\dot{L}_z < -\varepsilon_{\dot{L}_z}$	$\pm\varepsilon_{\dot{\theta}_g}$	$\pm\varepsilon_{F_x}$	$\pm\varepsilon_{F_y}$	$F_z < -\varepsilon_{F_z}$	$\pm\varepsilon_{T_x}$	$\pm\varepsilon_{T_y}$	$\pm\varepsilon_{T_z}$	$\pm\varepsilon_{F_g}$
	5	Rotating (Sweeping)	RT	+	$\dot{\theta}_x > \lvert\varepsilon_{\dot{\theta}_x}\rvert$	$\dot{\theta}_y > \lvert\varepsilon_{\dot{\theta}_y}\rvert$	$\pm\varepsilon_{\dot{\theta}_z}$	$\pm\varepsilon_{\dot{L}_z}$	$\pm\varepsilon_{\dot{\theta}_g}$	$F_x > \lvert\varepsilon_{F_x}\rvert$	$F_y > \lvert\varepsilon_{F_y}\rvert$	$\pm\varepsilon_{F_z}$	$T_x > \lvert\varepsilon_{T_x}\rvert$	$T_y > \lvert\varepsilon_{T_y}\rvert$	$\pm\varepsilon_{T_z}$	$\pm\varepsilon_{F_g}$
II	6	Closing - Pulling	CL-PL	+	$\pm\varepsilon_{\dot{\theta}_x}$	$\pm\varepsilon_{\dot{\theta}_y}$	$\pm\varepsilon_{\dot{\theta}_z}$	$\dot{L}_z > \varepsilon_{\dot{L}_z}$	$\dot{\theta}_g > \varepsilon_{\dot{\theta}_g}$	$\pm\varepsilon_{F_x}$	$\pm\varepsilon_{F_y}$	$F_z > \varepsilon_{F_z}$	$\pm\varepsilon_{T_x}$	$\pm\varepsilon_{T_y}$	$\pm\varepsilon_{T_z}$	$F_g > \varepsilon_{F_g}$
	7	Closing - Pushing	CL-PS	+	$\pm\varepsilon_{\dot{\theta}_x}$	$\pm\varepsilon_{\dot{\theta}_y}$	$\pm\varepsilon_{\dot{\theta}_z}$	$\dot{L}_z < -\varepsilon_{\dot{L}_z}$	$\dot{\theta}_g > \varepsilon_{\dot{\theta}_g}$	$\pm\varepsilon_{F_x}$	$\pm\varepsilon_{F_y}$	$F_z < -\varepsilon_{F_z}$	$\pm\varepsilon_{T_x}$	$\pm\varepsilon_{T_y}$	$\pm\varepsilon_{T_z}$	$F_g > \varepsilon_{F_g}$
	8	Closing - Rotating	CL-RT	+	$\dot{\theta}_x > \lvert\varepsilon_{\dot{\theta}_x}\rvert$	$\dot{\theta}_y > \lvert\varepsilon_{\dot{\theta}_y}\rvert$	$\pm\varepsilon_{\dot{\theta}_z}$	$\pm\varepsilon_{\dot{L}_z}$	$\dot{\theta}_g > \varepsilon_{\dot{\theta}_g}$	$F_x > \lvert\varepsilon_{F_x}\rvert$	$F_y > \lvert\varepsilon_{F_y}\rvert$	$\pm\varepsilon_{F_z}$	$\pm\varepsilon_{T_x}$	$\pm\varepsilon_{T_y}$	$\pm\varepsilon_{T_z}$	$F_g > \varepsilon_{F_g}$
	9	Pushing - Opening	PS-OP	+	$\pm\varepsilon_{\dot{\theta}_x}$	$\pm\varepsilon_{\dot{\theta}_y}$	$\pm\varepsilon_{\dot{\theta}_z}$	$\dot{L}_z < -\varepsilon_{\dot{L}_z}$	$\dot{\theta}_g < -\varepsilon_{\dot{\theta}_g}$	$\pm\varepsilon_{F_x}$	$\pm\varepsilon_{F_y}$	$F_z < -\varepsilon_{F_z}$	$\pm\varepsilon_{T_x}$	$\pm\varepsilon_{T_y}$	$\pm\varepsilon_{T_z}$	$F_g < -\varepsilon_{F_g}$
	10	Pushing - Rotating	PS-RT	+	$\dot{\theta}_x > \lvert\varepsilon_{\dot{\theta}_x}\rvert$	$\dot{\theta}_y > \lvert\varepsilon_{\dot{\theta}_y}\rvert$	$\pm\varepsilon_{\dot{\theta}_z}$	$\dot{L}_z < -\varepsilon_{\dot{L}_z}$	$\pm\varepsilon_{\dot{\theta}_g}$	$F_x > \lvert\varepsilon_{F_x}\rvert$	$F_y > \lvert\varepsilon_{F_y}\rvert$	$F_z < -\varepsilon_{F_z}$	$\pm\varepsilon_{T_x}$	$\pm\varepsilon_{T_y}$	$\pm\varepsilon_{T_z}$	$\pm\varepsilon_{F_g}$
	11	Rotating - Opening	RT-OP	+	$\dot{\theta}_x > \lvert\varepsilon_{\dot{\theta}_x}\rvert$	$\dot{\theta}_y > \lvert\varepsilon_{\dot{\theta}_y}\rvert$	$\pm\varepsilon_{\dot{\theta}_z}$	$\pm\varepsilon_{\dot{L}_z}$	$\dot{\theta}_g < -\varepsilon_{\dot{\theta}_g}$	$F_x > \lvert\varepsilon_{F_x}\rvert$	$F_y > \lvert\varepsilon_{F_y}\rvert$	$\pm\varepsilon_{F_z}$	$T_x > \lvert\varepsilon_{T_x}\rvert$	$T_y > \lvert\varepsilon_{T_y}\rvert$	$\pm\varepsilon_{T_z}$	$F_g < -\varepsilon_{F_g}$
III	12	Closing - Pulling - Rotating	CL-PL-RT	+	$\dot{\theta}_x > \lvert\varepsilon_{\dot{\theta}_x}\rvert$	$\dot{\theta}_y > \lvert\varepsilon_{\dot{\theta}_y}\rvert$	$\pm\varepsilon_{\dot{\theta}_z}$	$\dot{L}_z > \varepsilon_{\dot{L}_z}$	$\dot{\theta}_g > \varepsilon_{\dot{\theta}_g}$	$F_x > \lvert\varepsilon_{F_x}\rvert$	$F_y > \lvert\varepsilon_{F_y}\rvert$	$F_z > \varepsilon_{F_z}$			$\pm\varepsilon_{T_z}$	$F_g > \varepsilon_{F_g}$
	13	Closing -Pushing - Rotating	CL-PS-RT	+	$\dot{\theta}_x > \lvert\varepsilon_{\dot{\theta}_x}\rvert$	$\dot{\theta}_y > \lvert\varepsilon_{\dot{\theta}_y}\rvert$	$\pm\varepsilon_{\dot{\theta}_z}$	$\dot{L}_z < -\varepsilon_{\dot{L}_z}$	$\dot{\theta}_g > \varepsilon_{\dot{\theta}_g}$	$F_x > \lvert\varepsilon_{F_x}\rvert$	$F_y > \lvert\varepsilon_{F_y}\rvert$	$F_z < -\varepsilon_{F_z}$	$T_x > \lvert\varepsilon_{T_x}\rvert$	$T_y > \lvert\varepsilon_{T_y}\rvert$	$\pm\varepsilon_{T_z}$	$F_g > \varepsilon_{F_g}$
	14	Pushing - Rotating - Opening	PS-RT-OP	+	$\dot{\theta}_x > \lvert\varepsilon_{\dot{\theta}_x}\rvert$	$\dot{\theta}_y > \lvert\varepsilon_{\dot{\theta}_y}\rvert$	$\pm\varepsilon_{\dot{\theta}_z}$	$\dot{L}_z < -\varepsilon_{\dot{L}_z}$	$\dot{\theta}_g < -\varepsilon_{\dot{\theta}_g}$	$F_x > \lvert\varepsilon_{F_x}\rvert$	$F_y > \lvert\varepsilon_{F_y}\rvert$	$F_z < -\varepsilon_{F_z}$	$\pm\varepsilon_{T_x}$	$\pm\varepsilon_{T_y}$	$\pm\varepsilon_{T_z}$	$F_g < -\varepsilon_{F_g}$

Table 1: *Definitions of the 14 states based on spherical coordinate system with an origin at the port. Each state is characterized by a unique set of angular and linear velocities, forces, and torques. A non-zero threshold value is defined for each parameter by* ε *. The states' definitions are independent from the tool tip being used e.g. the state defined as Closing Handle might be associated with grasping or cutting if a grasper or scissors are being used respectively.*